

Identification and rejection of scattered neutrons in AGATA [☆]

M. Şenyiğit^{a,*}, A. Ataç^{a,b}, S. Akkoyun^c, A. Kaşkaş^a, D. Bazzacco^{d,e}, J. Nyberg^f, F. Recchia^{d,e}, S. Brambilla^g, F. Camera^{h,g}, F.C.L. Crespi^g, E. Farnea^{d,e,1}, A. Giaz^g, A. Gottardoⁱ, R. Kempley^j, J. Ljungvall^k, D. Mengoni^{d,l}, C. Michelagnoli^{d,e}, B. Million^g, M. Palacz^m, L. Pellegrini^{h,g}, S. Riboldi^{h,g}, E. Şahinⁱ, P.A. Söderström^{f,n}, J.J. Valiente Dobonⁱ, and the AGATA collaboration

^a*Department of Physics, Faculty of Science, Ankara University, TR-06100 Tandoğan, Ankara, Turkey*

^b*Department of Physics, Royal Institute of Technology, SE-10691 Stockholm, Sweden*

^c*Faculty of Science, Department of Physics, Cumhuriyet University, 58140 Sivas, Turkey*

^d*INFN Sezione di Padova, I-35131 Padova, Italy*

^e*Dipartimento di Fisica e Astronomia dell'Università di Padova, I-35131 Padova, Italy*

^f*Department of Physics and Astronomy, Uppsala University, SE-75120 Uppsala, Sweden*

^g*INFN Sezione di Milano, I-20133 Milano, Italy*

^h*Università degli Studi di Milano via Celoria 16, 20133, Milano, Italy*

ⁱ*Laboratori Nazionali di Legnaro, INFN, I-35020 Legnaro (PD), Italy*

^j*Department of Physics, University of Surrey, Guildford, GU2 7XH, UK*

^k*Centre de Spectrométrie Nucléaire et de Spectrométrie de Masse - CSNSM, CNRS/IN2P3 and Université Paris-Sud, F-91405 Orsay Campus, France*

^l*Nuclear Physics Research Group, University of West of Scotland, High Street, Paisley, PA1 2BE, Scotland, UK*

^m*Heavy Ion Laboratory, University of Warsaw, ul. Pasteura 5A, 02-093 Warszawa, Poland*

ⁿ*RIKEN Nishina Center, 2-1 Hirosawa, Wako-shi, Saitama 351-0198, Japan*

Abstract

Gamma rays and neutrons, emitted following spontaneous fission of ²⁵²Cf, were measured in an AGATA experiment performed at INFN Laboratori Nazionali di Legnaro in Italy. The setup consisted of four AGATA triple cluster detectors (12 36-fold segmented high-purity germanium crystals), placed at a distance of 50 cm from the source, and 16 HELENA BaF₂ detectors. The aim of the experiment was to study the interaction of neutrons in the segmented high-purity germanium detectors of AGATA and to investigate the possibility to discriminate neutrons and γ rays with the γ -ray tracking technique. The BaF₂ detectors were used for a time-of-flight measurement, which gave an independent discrimination of neutrons and γ rays and which was used to optimise the γ -ray tracking-based neutron rejection methods. It was found that standard γ -ray tracking, without any additional neutron rejection features, eliminates effectively most of the interaction points due to recoiling Ge nuclei after elastic scattering of neutrons. Standard tracking rejects also a significant amount of the events due to inelastic scattering of neutrons in the germanium crystals. Further enhancements of the neutron rejection was obtained by setting conditions on the following quantities, which were evaluated

[☆]In memory of Enrico Farnea

*Corresponding author

Email address: meneksek@science.ankara.edu.tr (M. Şenyiğit)

¹Deceased

for each event by the tracking algorithm: energy of the first and second interaction point, difference in the calculated incoming direction of the γ ray, figure-of-merit value. The experimental results of tracking with neutron rejection agree rather well with GEANT4 simulations.

Keywords: AGATA, Gamma-Ray Tracking, Segmented HPGe Detectors, Time-of-Flight (TOF), Neutron Scattering, Neutron-Gamma Discrimination, GEANT4 Simulations, ^{252}Cf .

1. Introduction

Fast neutrons emitted in nuclear reactions can travel long distances and may deposit part or all of their energies in the sensitive regions of the detectors, which are used for example for detection of γ rays. An investigation of neutron interactions in γ -ray tracking spectrometers, like AGATA [1] and GRETA/GRETINA [2–4], which are based on segmented high-purity germanium (HPGe) crystals, is of special interest for two reasons. First, an understanding of the neutron interactions can help to determine, quantify and reduce the neutron-induced background in the γ -ray spectra. This is the subject of the present work. Second, if the neutron interactions can be detected and identified as such, it may be possible to use the γ -ray spectrometer also as a neutron detector, with an efficient detection of the number of emitted neutrons in the nuclear reactions.

In an earlier GEANT4 [5, 6] simulation of the 4π AGATA γ -ray spectrometer, it was shown that fast neutrons, with energies between 0.5 MeV and 10 MeV, interact on average 7 times with the germanium nuclei in the AGATA crystals and eventually either escape from the array or become absorbed through neutron capture [7]. It was also estimated that, in the same energy range, the probability of detecting neutrons by AGATA is about 50% assuming a low-energy threshold of 5 keV. In the same work, the influence of neutron interactions on the γ -ray tracking algorithms was investigated, observing that the neutron-induced background reduces the sensitivity of the spectrometer. This background may become a serious problem in future experiments with neutron-rich radioactive ion beams, when used in reactions in which a large number of neutrons are emitted and in experiments where the cleanliness of the γ -ray spectra is of utmost concern.

Different approaches can be used to discriminate neutrons and γ rays in segmented HPGe detectors, the most obvious one making use of the time-of-flight (TOF) difference between neutrons and γ rays. At the nominal source to detector distance, which is 23.5 cm for the AGATA spectrometer, or at shorter distances, this approach is expected to be of limited use due to the time resolution of the germanium detectors. Another approach is to make use of

the detector segmentation, either in the γ -ray tracking [7, 8] or pulse-shape analysis procedures. Non-segmented HPGe detectors did not show any difference in the pulse shapes of neutrons and γ rays [9]. However, segment information may improve this approach, as suggested by Jenkins et al. [10], where the inelastic excitation and the subsequent decay of the 0^+ isomer in ^{72}Ge was exploited to tag neutrons by making use of the pulse-shape analysis. Identification of the neutron interaction points in a segmented HPGe detector was also investigated by Abt et al. [11], with the aim of reducing the neutron-induced background.

In a previous simulation of AGATA, three methods were developed, based on γ -ray tracking for rejection of the neutron-induced background in the γ -ray spectra [8]. These methods made use of the energy of the first and second interaction point, the incoming direction of the γ ray and the figure-of-merit value of γ -ray tracking algorithm. The promising results of the simulations are here tested with real experimental data obtained with the AGATA spectrometer. The neutron rejection power of each method is quantified and different combinations of the methods are investigated in order to improve the technique. The experimental setup of this work is specially designed to get a clear identification of neutrons by utilising the TOF method, which is achieved by having a large distance between the source and the AGATA detectors and by using BaF₂ detectors as time reference. The TOF results are used to optimise the neutron rejection methods based on γ -ray tracking.

2. Experiment and data analysis

The experiment was carried out during the experimental campaign of AGATA at INFN Laboratori Nazionali di Legnaro (LNL), Italy [12, 13]. A schematic picture of the experimental setup is shown in Fig. 1. A 60 kBq ^{252}Cf source was placed at a distance of about 50 cm from the front face of four AGATA triple cluster (ATC) detectors [14], each containing three encapsulated 36-fold segmented n-type HPGe crystals. For the measurement of the TOF of neutrons and γ rays, 16 BaF₂ scintillator detectors (hexagonal shape, 2 inch diameter,

3 inch length) from the HELENA detector array were placed in two groups on each side of the ^{252}Cf source at a distance of about 14 cm. In order to increase the relative yield of neutrons compared to γ rays hitting the ATC detectors, a lead shield with a thickness of 5 cm was placed between the ^{252}Cf source and the ATC detectors. The shield reduced the γ rays and neutrons by about 95 % and 50 %, respectively.

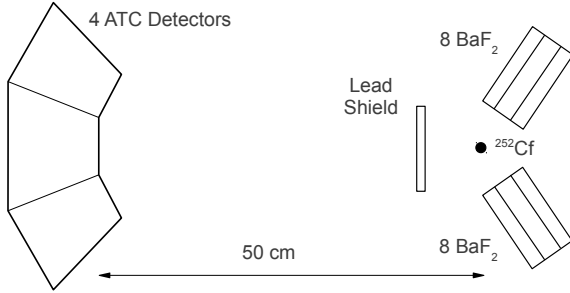


Figure 1: Schematic picture of the experimental setup.

A hardware trigger condition was made in the following way. The preamplifier core signal of each of the 12 HPGe crystals, obtained from the signal inspection output of the AGATA digitisers, was fed into an analog timing filter amplifier and further into an analog constant fraction discriminator (CFD). The CFD thresholds on the HPGe core signals were set as low as possible, with values ranging from 10 keV to 20 keV. A logical OR of the HPGe core CFD signals was created. The BaF₂ anode signals were fed into a BaF₂ signal processor unit [15], which produced a logical OR of the CFD signals from each BaF₂ detector. The hardware trigger signal was made as an AND of the HPGe OR and the BaF₂ OR signals, i.e. at least one HPGe core signal and at least one BaF₂ anode signal was required to produce an event. The hardware trigger signal was sent to the AGATA Global Trigger and Synchronisation (GTS) system via the AGATA VME/VXI interface (AGAVA).

For each HPGe crystal, which contributed to the trigger (core signal above threshold and in coincidence with HELENA), the pre-processing electronics produced the following data for readout for the core and for all 36 segments: energy, timestamp, and 100 sampling points (1000 ns) of the leading edge of the digitised waveforms. No low-energy thresholds were applied by the hardware on the HPGe segment signals: for each crystal, the data from all 36 segment signals were readout whenever a core signal was present. The energy and time of each BaF₂ detector signal were processed by VME ADCs and TDCs and readout via the AGAVA interface. A detailed description of the AGATA detectors, their electronics and the data acquisition system can be found

elsewhere [1].

The singles HPGe core and BaF₂ rates were about 200 Hz and 500 Hz per detector, respectively, and the trigger rate was about 120 Hz. The experiment lasted for about 3 days, during which a total of 5.3×10^6 events were collected.

A ^{60}Co source calibration, with 3 ATC detectors placed at a distance of 50 cm, was performed before the ^{252}Cf experiment. The ^{60}Co dataset contained about 1.0×10^6 events and was used to test the influence of the neutron-gamma discrimination methods on data containing no neutron events.

The three-dimensional positions of the interaction points were obtained by pulse-shape analysis (PSA) of the recorded signal waveforms using the adaptive grid-search algorithm [16]. The signal basis used by the PSA algorithm was obtained from the AGATA Detector Simulation Software ADL (the version used was from 2010-07-28) [17]. It should be noted that the adaptive grid-search algorithm works very well as long as there is only one interaction point per crystal. It can also handle multiple interactions in the same crystal if the transient signals of the segments do not overlap [1].

In the replay, a digital CFD algorithm was applied on the core signal waveforms, to calculate the HPGe core time. The low-energy threshold applied by this algorithm was about 10 keV. A TOF parameter was created as the time difference between the HPGe core time and the average BaF₂ time, obtained as an average of the BaF₂ detector times within a narrow time window.

2.1. Gamma-ray tracking

Gamma-ray tracking was performed by the `mgT` code [18] that uses the so-called forward tracking method [19, 20], which is based on the clusterisation of interaction points belonging to the same initial γ ray. Among many possible clusters, the tracking code finds and selects only the one with the best (smallest) figure-of-merit (FM) value. The FM calculation is based on a comparison of the energy of the scattered γ rays calculated 1) by using the interaction point energies and 2) by applying the Compton scattering formula to the positions of the interaction points. The probabilities of photoelectric effect, Compton scattering and pair production, as well as the probability for the γ ray to travel the measured distances between the interaction points in a cluster, are included in the FM calculation.

The programs `GF3` [21] and `ROOT` [22] were used for the analysis of tracked γ -ray and other histograms.

2.2. Tracking efficiency and peak-to-total ratio

A parameter of the `mgt` code that has an important effect on the tracking results is the so-called `lim` parameter, which gives an upper limit for the FM value. Clusters with larger FM values than `lim` are either restructured or rejected. Depending on the chosen `lim` value, either a high tracking efficiency or a large peak-to-total (P/T) ratio is obtained. The selection of the `lim` value can be done by using a dataset obtained with a ^{60}Co source. The P/T ratio is defined as the ratio of the sum of counts in the 1173 keV and 1332 keV peaks to the sum of counts in the total spectrum, integrated from zero energy or from a low-energy threshold to just above the 1332 keV peak. The tracking efficiency is the ratio of the sum of counts of the two peaks in the tracked γ -ray spectrum to the sum of counts of the peaks in a spectrum created from the core signals.

The results obtained from an analysis of the ^{60}Co dataset, by using different `lim` values, are shown in Table 1. In the present work, γ -ray tracking performed by using `lim = 0.02` and none of the tracking methods for neutron rejection (see subsection 3.2.2), is called “standard tracking”, since it gives a tracking efficiency and a P/T value that are closest to what was reported earlier for a setup with three ATC detectors [1]. Note that for the largest three `lim` values shown in the table, basically all clusters are accepted by `mgt`, giving more counts in the ^{60}Co peaks as well as increasing the background in the γ -ray spectra. This explains the large tracking efficiency values, even above 100 %, and the small P/T values.

2.3. Neutrons and gamma rays emitted by ^{252}Cf

The average prompt neutron and γ -ray multiplicity per ^{252}Cf fission are about 3.8 and 8, respectively. The neutrons have an energy distribution peaking between 0.5 MeV and 1 MeV, extending to about 10 MeV, and has an average value of 2.14 MeV. For detailed information about the γ -ray and neutron emission from ^{252}Cf , see e.g. Refs. [23–26].

2.4. Cross sections for neutron capture on $^{\text{nat}}\text{Ge}$

In the neutron energy interval of interest, which is from 1 MeV to 10 MeV, the total cross section for neutrons on $^{\text{nat}}\text{Ge}$ is in the range from 3.4 barn to 4.6 barn [27, 28]. At 2.14 MeV the total, elastic and inelastic cross sections for neutrons on $^{\text{nat}}\text{Ge}$ are 3.4 barn, 2.2 barn, and 1.0 barn, respectively [27, 28]. The cross sections for other reaction channels are much smaller (0.2 barn).

After elastic or inelastic scattering of 2 MeV neutrons, the energy deposited in a HPGe detector by the recoiling Ge nuclei has a maximum value of about 100 keV [8, 9]. Due to the pulse-height defect [23], this energy is reduced to about 35 keV [9]. In the case of inelastic scattering, both the Ge-recoil energy and parts or all of the γ -ray energy, originating from the de-excitation of the excited Ge isotopes, are deposited in the detectors.

2.5. Distribution of number of interaction points for neutrons and gamma rays

By using the TOF parameter, the distribution of the number of interaction points (npt) can be obtained separately for neutrons and γ rays. The average npt values obtained for the TOF-gated distribution was 2.35 for neutrons, 1.84 for γ rays and 1.96 for the un-gated case (see subsection 3.1 for a description of the TOF gates). For the 4π AGATA array the npt values for neutrons are expected to be significantly larger, while they will remain essentially unchanged for γ rays.

There is a large excess of events with $npt = 1$, which mainly correspond to elastic scattering of neutrons and small angle Compton scattering of γ rays. Standard tracking rejects about 75 % of the single interaction points, since they do not qualify as photo-absorption points and consequently their FM values are not good enough. The rest of the single interaction points give rise to single-hit clusters. The average value of the number of interaction points in a cluster ($nptc$) after tracking with `mgt` was 2.78 for neutrons, 2.11 for γ rays and 2.23 for the un-gated distribution.

2.6. Identification of gamma-ray peaks

Due to the 5 cm thick lead block used in the experiment, γ rays which originate from the ^{252}Cf source are highly reduced in the spectra shown in Fig. 2. The strongest peaks observed are the ones which originate from the de-excitation of the different Ge isotopes and from the material surrounding the setup. Transitions due to the de-excitation of the lowest lying states of these isotopes are visible both in the core and in the tracked γ -ray energy spectra. The 596 keV, 608 keV and 1204 keV peaks originate from the $2_1^+ \rightarrow 0_1^+$, $2_2^+ \rightarrow 2_1^+$ and $2_2^+ \rightarrow 0_1^+$ transitions, respectively, in ^{74}Ge . The 563 keV and 847 keV peaks are due to the $2_1^+ \rightarrow 0_1^+$ and $4_1^+ \rightarrow 2_1^+$ transitions, respectively, in ^{76}Ge . The 834 keV peak is due to the $2_1^+ \rightarrow 0_1^+$ transition in ^{72}Ge and the 1040 keV peak is due to the

Table 1: The dependency of tracking efficiency and peak-to-total on the l_{im} parameter of the `mgt` tracking program. The values listed are for the 1173 keV and 1332 keV peaks and were obtained in a measurement with three ATC detectors placed at a distance of 50 cm from the ^{60}Co source. The values in the column “No threshold” were obtained by setting no additional software threshold on the data, while the values in the column “200 keV threshold” were obtained by setting a software threshold at 200 keV. To enable a comparison of results obtained in previous works [1], only events with more than one interaction point were analysed. The P/T value of a γ -ray spectrum that was created from the core signals was 16.66(7)%. No background subtraction was performed. Errors given are purely statistical.

l_{im}	Tracking efficiency [%]	Peak-to-total (P/T) [%]	
		No threshold	200 keV threshold
10	104.7(8)	41.5(2)	42.2(2)
1	103.3(6)	44.7(2)	45.2(2)
0.5	102.1(6)	46.1(2)	46.6(2)
0.1	96.8(5)	50.8(2)	51.1(2)
0.05	92.9(5)	53.4(2)	53.6(2)
0.03	89.0(5)	55.5(3)	55.7(3)
0.02	85.4(5)	57.4(3)	57.6(3)
0.01	77.1(4)	60.9(3)	61.1(3)

$2_1^+ \rightarrow 0_1^+$ transition in ^{70}Ge . The 690 keV γ ray originates from the de-excitation of the first 0^+ excited state ($t_{1/2} = 444$ ns) to the 0^+ ground state of ^{72}Ge . Since the 690 keV peak is due to the detection of conversion electrons, it is strongly reduced in the tracked γ -ray spectrum (the tracking algorithm does not include the process of emission of conversion electrons).

The small bumps observed at 1464 keV and 1711 keV most likely have contributions from more than one γ -ray transition in $^{70,72,74}\text{Ge}$. It is estimated that the 1464 keV γ ray (^{72}Ge) gives the largest contribution to the first bump, whereas the 1708 keV (^{70}Ge) and 1711 keV (^{72}Ge) γ rays give the largest contribution to the second one.

On the high-energy side of the γ -ray peaks, originating from the $^{70,72,74,76}\text{Ge}(n,n'\gamma)$ reactions, about 40 keV wide bumps, are observed. They appear clearly in the core-energy spectrum, because the Ge-recoil energies are added to the energies of the transitions following the $^{\text{nat}}\text{Ge}(n,n'\gamma)$ reaction. The bumps are smaller but still visible in the tracked spectrum. This can be explained considering that the interaction points due to the Ge recoils are sometimes included in the `mgt` clusters and their energies are added to the peak energies.

The peaks at 847 keV, 1436 keV and 2615 keV are related to the transitions following the $^{56}\text{Fe}(n,n'\gamma)$, $^{138}\text{Ba}(n,n'\gamma)$ and $^{208}\text{Pb}(n,n'\gamma)$ reactions in the iron material close to the experimental setup, in the BaF_2 detectors and in the lead block, respectively. The peaks at 844 keV, 1014 keV and 2211 keV are identified as transitions following the $^{27}\text{Al}(n,n'\gamma)$ reac-

tion. Since the 2212 keV level in ^{27}Al has a short mean life (26.6 fs [29]), the peak marked at 2211 keV is Doppler broadened [30] with a FWHM value of 15 keV. Due to the natural background radioactivity, the ^{214}Pb peak at 352 keV, the ^{214}Bi peaks at 1120 keV, 1238 keV, 1765 keV and the ^{40}K peak at 1461 keV are observed in this spectrum as a result of random coincidences.

The counts at low energy, below 45 keV, which are mainly due to the recoiling Ge nuclei after elastic scattering of neutrons, are effectively removed from the tracked spectra, as seen in Fig. 2. These type of interactions give rise to single-hit clusters, which are rejected during the γ -ray tracking process (see subsection 2.5). The low-energy bump which appears between 50 keV and 250 keV in the tracked spectrum originates from single interaction points with accepted FM values. The bump disappears completely in the red spectrum, for which single-hit clusters with $n_{ptc} = 1$ were rejected.

3. Neutron-gamma discrimination

In this section, the different neutron-gamma discrimination methods are compared.

3.1. Time-of-flight

A simple and straightforward method for neutron- γ discrimination is to use the difference in TOF of neutrons and γ rays. This method can be successful if the time resolution of the detectors is good enough and if the variation in flight distance, due to the finite

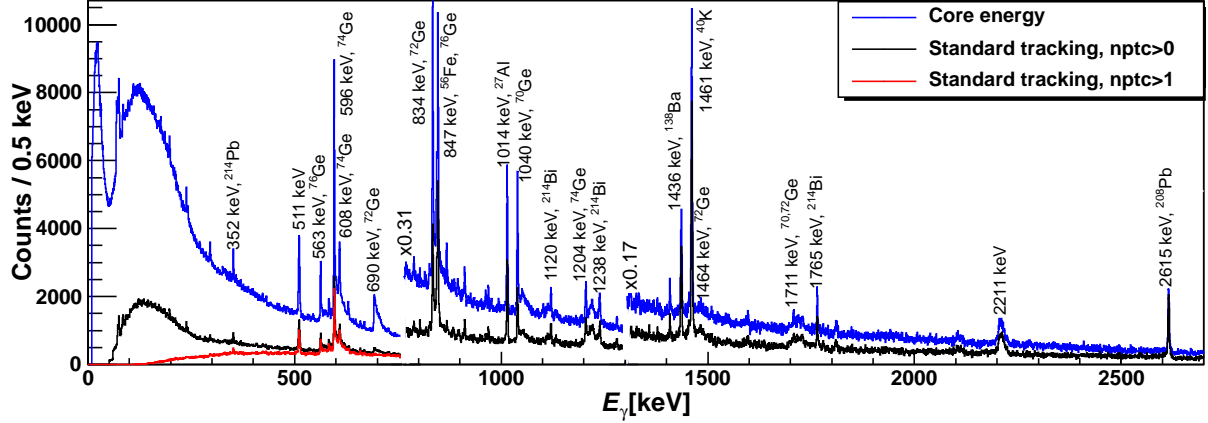


Figure 2: (Colour online) Energy spectra measured with four ATC detectors and the ^{252}Cf source. The black and red spectra are obtained after γ -ray tracking including all events ($n_{\text{ptc}} > 0$) and including only events with more than one interaction point ($n_{\text{ptc}} > 1$), respectively. The blue spectrum is the sum of the core energies from the detectors.

detector thickness, is small enough for the neutron energy range of interest.

The histograms in Fig. 3 show a) TOF as a function of the energy of the interaction points deposited in the Ge crystals and b) TOF as a function of the tracked γ -ray energy using standard tracking. In Fig. 3a, γ rays due to inelastic scattering of neutrons on different Ge isotopes can be seen at 596 keV (^{74}Ge) and at 834 keV (^{72}Ge) for TOF values larger than about 10 ns. In the region of low energies ($E_{\text{int}} \lesssim 45$ keV) and large TOF values ($\gtrsim 10$ ns), interaction points due to recoiling Ge nuclei after elastic and inelastic scattering of neutrons can be seen. The 690 keV γ ray (^{72}Ge), which is due to the de-excitation of the 0^+ first excited state with a half life of 444 ns, is visible as a broad structure at large TOF values.

In Fig. 3b, the 596 keV, 834 keV, 1040 keV, 1204 keV, 1464 keV and 1708 keV γ rays, which follow the $^{\text{nat}}\text{Ge}(n,n'\gamma)$ reactions, are observed at TOF values larger than about 10 ns, together with their bumps on the high-energy side of the peaks. The 1014 keV γ ray, following the $^{27}\text{Al}(n,n'\gamma)$ reaction, is observed both at small and large TOF values. Aluminium can be found in a number of places in the experimental area both at short and long distances from the ^{252}Cf source, e.g. in the detector capsules, which leads to large distances and long neutron flight times, and in the material that is located close to the ^{252}Cf source. The 1436 keV γ ray, which is emitted following the $^{138}\text{Ba}(n,n'\gamma)$ reaction, is visible at TOF values less than about 20 ns. This is expected due to the relatively short neutron flight distance for reaching the BaF_2 detectors. Finally, the 511 keV peak, mainly originating

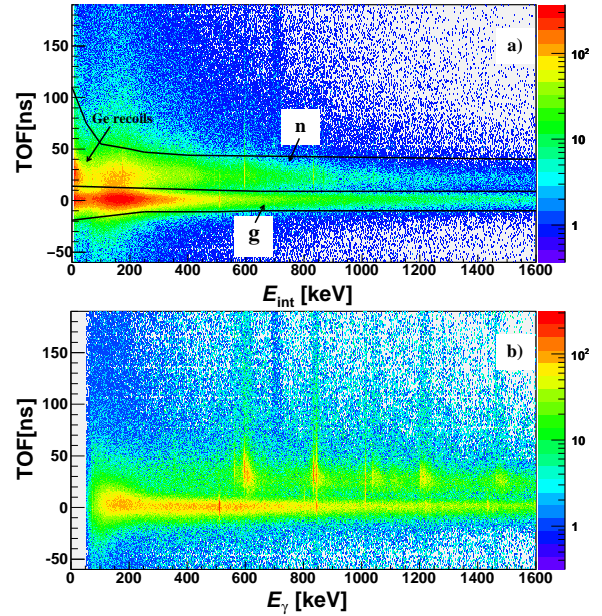


Figure 3: (Colour online) TOF (=time difference between the HPGe core and BaF_2 times) versus a) interaction point energy and b) tracked γ -ray energy using standard tracking, measured with the ^{252}Cf source. The two-dimensional gates shown in a) are used for gating on neutrons (n) and γ rays (g).

from pair-production and positron annihilation in the HPGe crystals, is clearly visible in Fig. 3b.

Two-dimensional TOF gates, indicated by n (neutrons) and g (γ rays) in Fig. 3a, were defined in order to make a TOF gated neutron- γ discrimination that was as clean as possible. For an mgt cluster to be qualified as a γ ray, all of its interaction points were required to be in the g gate. Fig. 4 shows tracked γ -ray spectra with no TOF gate and with a TOF gate on γ rays (gate g). It is clear from this figure that standard tracking alone cannot eliminate the neutron-induced peaks and their bumps. They are, however, effectively eliminated by using the TOF gate. As expected, the peaks at 511 keV, 847 keV, 1014 keV, 1436 keV, 2211 keV and 2615 keV, which originate from positron annihilations and from the reactions $^{56}\text{Fe}(n,n'\gamma)$, $^{27}\text{Al}(n,n'\gamma)$, $^{138}\text{Ba}(n,n'\gamma)$, $^{27}\text{Al}(n,n'\gamma)$ and $^{208}\text{Pb}(n,n'\gamma)$, respectively, are still visible after the TOF gating.

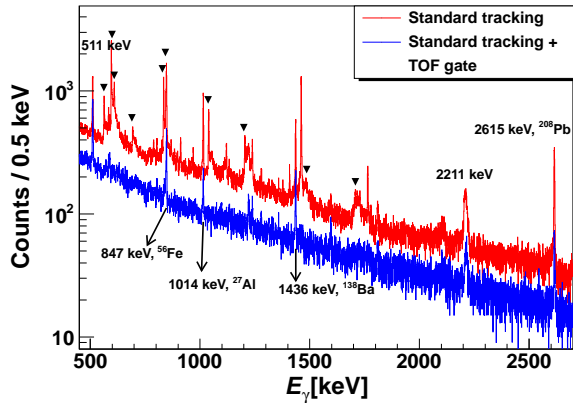


Figure 4: (Colour online) Gamma-ray energy spectra obtained with the ^{252}Cf source and by using standard γ -ray tracking without any TOF gate (red) and with a TOF gate on γ rays (blue; gate g in Fig. 3a). The 511 keV, 847 keV, 1014 keV, 1436 keV, 2212 keV and 2615 keV γ rays are emitted following positron annihilation and the reactions $^{56}\text{Fe}(n,n'\gamma)$, $^{27}\text{Al}(n,n'\gamma)$, $^{138}\text{Ba}(n,n'\gamma)$, $^{27}\text{Al}(n,n'\gamma)$ and $^{208}\text{Pb}(n,n'\gamma)$, respectively. The black triangles indicate γ rays due to inelastic scattering of neutrons on the stable Ge isotopes. The γ -gated spectrum (blue) contains 68% of the counts in the un-gated spectrum (red).

The time resolution of the AGATA detectors can be investigated as a function of interaction point energy by using the TOF histogram shown in Fig. 3a. Disregarding the time spent by γ rays traversing the length of the Ge crystal ($\lesssim 0.3$ ns) and the time resolution of the BaF_2 detectors (FWHM $\simeq 0.5$ ns), the width of the time peak due to γ rays projected on the y axis gives us an estimate of the time res-

olution of the AGATA detectors. The results are shown in Fig. 5, where TOF histograms are plotted for different gates on the interaction point energies. The time resolution is not so good for small interaction point energies due to small detector signals with worse signal-to-noise ratio. The γ rays give a time distribution with a centroid at 1.7 ns, which is the time it takes for γ rays to travel a distance of 50 cm. Since the flight time of the neutrons depends on their energies, wider TOF distributions are obtained for neutrons compared to γ rays. For $E_{\text{int}} < 35$ keV, the enhanced neutron TOF distribution is mainly due to recoiling Ge nuclei. In the range of interaction point energies from 100 keV to 1200 keV, the FWHM of the γ -ray time peak decreases slowly from 9.8 ns to 7.7 ns.

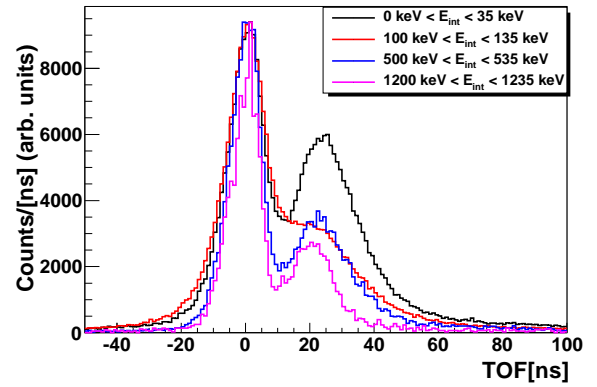


Figure 5: (Colour online) TOF histograms obtained with the ^{252}Cf source and with gates on different interaction point energy ranges. The histograms are normalised to have the same height of the peak due to γ rays.

The FWHM values given above for the AGATA detectors give a good neutron- γ discrimination at a source to AGATA distance of 50 cm. At the nominal distance of 23.5 cm the TOF method can be useful only if a better time resolution is obtained, e.g. by improving the PSA technique. This possibility was investigated by Crespi et al. [31] by using a small non-segmented HPGe detector.

3.2. Tracking

Neutron- γ discrimination based on standard tracking and on the three tracking methods which were developed for improved neutron rejection, are described in this subsection. These methods can be used instead of, or as a complementary to, the TOF method.

3.2.1. Standard tracking

As shown in Fig. 2, the low-energy interaction points ($E_{\text{int}} \lesssim 45$ keV), which are mainly due to the recoiling Ge nuclei after the elastic scattering of neutrons, are effectively removed from the spectra by γ -ray tracking. In addition, standard tracking also reduces the peaks and bumps due to inelastic scattering of the neutrons in the HPGe detectors.

In order to obtain quantitative values for the reduction of counts in the neutron-induced peaks and their associated bumps, the 1040 keV peak, which originates from the $^{70}\text{Ge}(n, n'\gamma)$ reaction, was selected. In the energy range of this peak and its bump (from 1035 keV to 1080 keV) the γ -ray spectra are clean with no other peaks. As a reference, the reduction of counts in the 1173 keV and 1332 keV peaks of ^{60}Co were also evaluated. A perfect neutron- γ discrimination would give a 100% reduction of the counts both in the peak and in the bump due to the 1040 keV transition, and no reduction (0%) of the counts in the 1173 keV and 1332 keV peaks. The results obtained with standard tracking were the following (see row 1 in Table 4): the 1040 keV peak was reduced by 57%, the 1040 keV peak plus its associated bump by 52%, while the 1173 keV and 1332 keV peaks of ^{60}Co were reduced by 9% and 12%, respectively.

3.2.2. Tracking with neutron rejection: description of methods

In order to improve the neutron rejection compared to what can be achieved by using standard tracking, three methods based on the γ -ray tracking were developed [8]. In this earlier work, the interaction of neutrons and γ rays in the AGATA detectors were simulated by using the GEANT4 toolkit [5, 6]. Three methods were established to distinguish between two types of γ rays: the ones that originate from the source and the ones that are produced in the detectors after inelastic scattering of neutrons, $^{\text{nat}}\text{Ge}(n, n'\gamma)$.

The first method is based on the idea that the energy deposited in the first interaction point ($E_{\text{int},1}$) is expected to be different for neutrons and γ rays. For neutron inelastic scattering, the first interaction point, which is due to the Ge recoil, has a low energy ($E_{\text{int}} \lesssim 35$ keV, for 2 MeV neutrons). If the first interaction point in an mgt cluster is identified correctly by the γ -ray tracking procedure, the rejection of mgt clusters with low $E_{\text{int},1}$ values can be a successful way of reducing neutron-induced events. Considering the possibility that the ordering of the interaction points in an mgt cluster may be wrong, or that there may be a neutron elastic scattering be-

fore the inelastic scattering, the energy of the second interaction points ($E_{\text{int},2}$) may also be used for neutron rejection.

The second method is based on the difference in the incoming direction of the γ rays, for which two different angles θ_G and θ_C , are defined [7, 32]. The geometric angle, θ_G , is the angle between the line passing through the position of the source and the first interaction point and the line passing through the first and the second interaction points. The Compton scattering angle, θ_C , is calculated from the Compton scattering formula using the position of the source, the total energy deposited by the γ ray and the energy of the first interaction point. If the incoming particle is a γ ray, the difference $\Delta\theta = \theta_G - \theta_C$ should be distributed with its centroid at 0° . The width of the distribution depends largely on the interaction position resolution [32, 33] and on the ability of the tracking algorithm to correctly assign the first and second interaction points. If the incoming particle is a neutron, the kinematics of the scattering will produce a different θ_C with respect to what is expected by the Compton scattering formula. A broader asymmetric $\Delta\theta$ distribution is expected, with a centroid that is not at 0° [8]. By setting a gate on $\Delta\theta$ it may be possible to improve the neutron rejection.

The third method is based on the selection of the FM value in the tracking code. The validity of a cluster is checked by using its FM value which is determined by the γ -ray interaction probabilities in Ge. If a cluster contains a neutron interaction point, it is expected to give a larger (worse) FM value compared to a cluster with only γ ray interaction points.

These three methods were tested in simulations of neutrons and γ rays emitted from the center of AGATA for different energy and multiplicity values with good results for the neutron rejection [8]. In the present work, these tracking methods were implemented in the mgt program and tested with real data.

3.2.3. Tracking with neutron rejection: results

The spectra in Fig. 6 show the distribution of the energies of the first ($E_{\text{int},1}$) and second ($E_{\text{int},2}$) interaction points for neutron and γ -ray events, selected by using the n and g TOF gates, respectively, shown in Fig. 3a. Both spectra, gated on neutrons, have large abundances of counts at low energy, below about 45 keV, compared to the spectra gated on γ rays. For example, by requiring $E_{\text{int},1} > 45$ keV and/or $E_{\text{int},2} > 45$ keV, it is possible to eliminate more of the neutron-induced events compared to the

events that are due to γ rays.

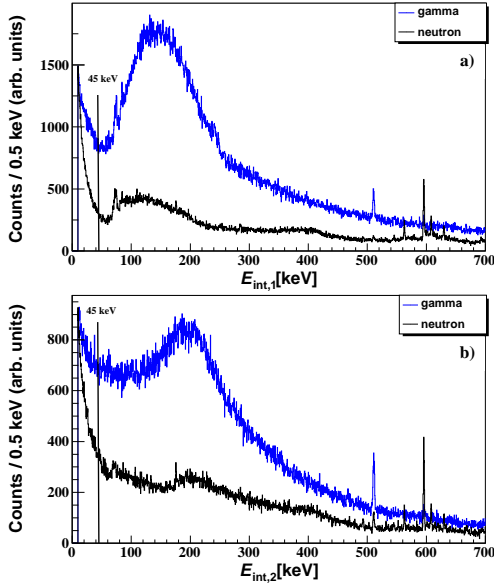


Figure 6: (Colour online) Distribution of the energy deposited in a) the first and b) the second interaction point by setting TOF gates on neutrons (black) and γ rays (blue) according to Fig. 3a. The spectra were obtained with the ^{252}Cf source and by using standard tracking. The spectra are normalised to have the same number of counts at 10 keV.

The distribution of the difference $\Delta\theta = \theta_G - \theta_C$ for neutrons and γ rays is shown in Fig. 7. As expected the distribution is centered at 0° for γ rays, while a broader and asymmetric distribution is observed for neutrons. The two distributions are not so different and a gate on $\Delta\theta$ for rejection of neutron events, without losing too many good γ -ray events, is not trivial. Different values of the gate on $\Delta\theta$ were tested and as a compromise $\Delta\theta < 40^\circ$ was selected for the further analysis below.

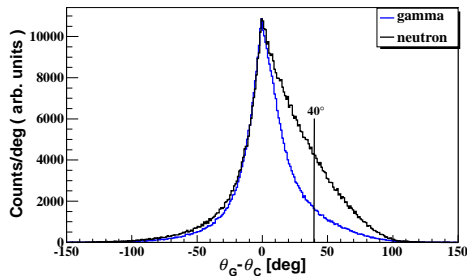


Figure 7: (Colour online) Distribution of $\Delta\theta = \theta_G - \theta_C$ for neutrons (black) and γ rays (blue) obtained with the ^{252}Cf source. The neutrons and γ rays were selected by using the TOF gates n and g, respectively, shown in Fig. 3a. The spectra are normalised to have the same number of counts at the maximum of the peaks.

The distribution of FM values for neutrons and γ rays are shown in Fig. 8 in the range from 0 to 0.02. In this work, the largest allowed FM value was 0.02, which corresponds to the 1 μm value defined as standard tracking (see section 2.2). There is almost no difference between the FM distributions for neutrons and γ rays when events with any $nptc$ values are included (Fig. 8a). The distributions for events with $nptc > 1$ (Fig. 8b) show, however, that the neutron induced events tend to have larger FM values. Different FM values in the range from 0 to 0.02 were tested, both for events with $nptc > 0$ and $nptc > 1$, by analysing tracked γ -ray spectra and by evaluating the rejection of neutron-induced events in the ^{252}Cf dataset compared to rejection of γ -ray events in the ^{60}Co dataset. The results of this evaluation led to the conclusion that an FM value < 0.01 was optimal for the present work. This is the value used in the further analysis below.

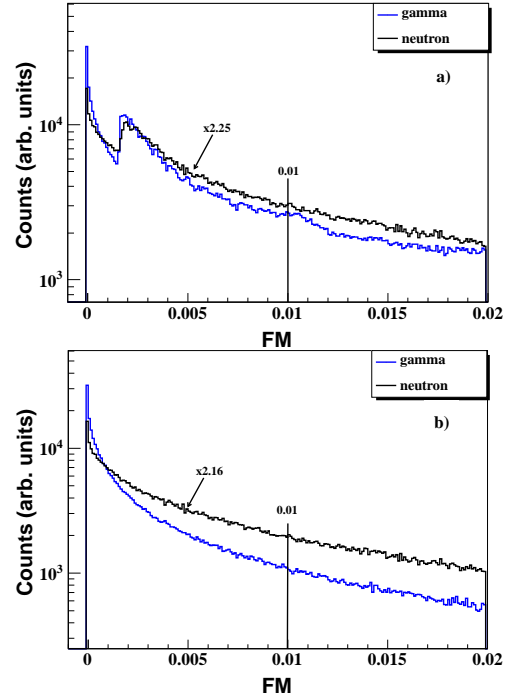


Figure 8: (Colour online) Distribution of the figure-of-merit (FM) of the mgt clusters for data taken with the ^{252}Cf source for a) all events and b) events with $nptc > 1$. The blue spectrum is obtained by gating on the γ rays and black spectrum by gating on neutrons using the TOF gates show in Fig. 3a. The blue and black histograms are normalised to have the same number of counts in the range of FM values from 0.4×10^{-3} to 1.7×10^{-3} .

Different combinations of gates on $E_{\text{int},1}$, $E_{\text{int},2}$, $\Delta\theta$ and FM were tested in order to obtain the best neutron- γ discrimination. Quantitative results are given in Table 2. The peak at 1040 keV ($2^+ \rightarrow 0^+$

transition in ^{70}Ge) and its bump were analysed in tracked spectra obtained from the ^{252}Cf dataset, before and after different combinations of the four gates were applied. The 1173 keV and 1332 keV peaks of the ^{60}Co dataset were analysed in the same way. The aim was to find the gate combinations, which reduce the number of counts in the neutron-induced 1040 keV peak and its bump as much as possible, while keeping the number of counts in the ^{60}Co peaks as large as possible. The gate combinations that caused a loss of more than 20 % of the counts in the 1332 keV peak of ^{60}Co were disregarded.

An example of a good gate combination is an OR of the following conditions: $E_{\text{int},1} > 30 \text{ keV}$, $E_{\text{int},2} > 30 \text{ keV}$, $\Delta\theta < 40^\circ$, $FM < 0.01$. This gate combination reduces the 1040 keV transition by 28 %, the 1040 keV transition together with its bump by 42 % and the total spectrum from 0 keV to 4095 keV by 34 %, compared to the spectrum obtained by standard tracking. This caused a loss of 19 % of the counts in the 1332 keV peak of ^{60}Co . An investigation of correlations between the gating parameters, which could be used to further improve the neutron rejection, was also made. This was done by producing two-dimensional histograms of the parameters, e.g. $E_{\text{int},1}$ versus $\Delta\theta$ or $E_{\text{int},1}$ versus FM , and by setting two-dimensional gates in such histograms. No apparent improvement of the neutron rejection was obtained in this way.

In order to compare the experimental results with simulations, a simulation was carried out with the AGATA GEANT4 code [6] using a setup with four ATC detectors placed at a distance of 50 cm from the ^{252}Cf and ^{60}Co sources. The simulation was performed as described in detail in Ref. [8], except that the number of ATCs and the distance to the source was different. Tracking was performed by using $lim = 0.02$ and two different low-energy thresholds, 5 keV and 10 keV. The results of the simulation are given in Table 3. By using a low-energy threshold of 10 keV and the gate combination [$E_{\text{int},1} > 30 \text{ keV}$ OR $E_{\text{int},2} > 30 \text{ keV}$ OR $\Delta\theta < 40^\circ$ OR $FM < 0.01$], the counts in the 1040 keV peak was reduced by 25 %, in the 1040 keV peak and its associated bump by 39 % and in the total spectrum (0 keV to 4095 keV) by 43 %, as compared to the spectrum obtained by standard tracking. This caused a loss of 12 % of the counts in the 1332 keV peak.

The effect of varying the low-energy threshold was tested by reducing the value to 5 keV, which gave a significant improvement of the neutron rejection. In this case, with the same gate combination and having nearly the same loss of counts in the 1332 keV

peak, the counts in the 1040 keV peak was reduced by 28 %, in the peak plus the bump by 57 % and in the total spectrum by 51 %, as compared to the spectrum obtained by standard tracking.

The experimental results are in rather good agreement with the results of the simulation obtained by using a low-energy threshold of 10 keV (compare the results in Table 2 and 3). The experimental results are slightly worse than the simulated results, in particular regarding the reduction of the counts in the 1332 keV peak of ^{60}Co . It is likely that the experimental results can become better by improving the PSA techniques to give more precise interaction positions and better identification of multiple hits in the same crystal. Note that, with such an improvement, it may be possible to use only one or two of the gates, e.g. the combination [$E_{\text{int},1} > 30 \text{ keV}$ OR $\Delta\theta < 40^\circ$], to obtain a reasonable reduction of the neutron-induced background without losing efficiency in the ^{60}Co peaks.

Since the TOF method gives an excellent neutron rejection, the γ -ray spectrum obtained by using the TOF gate is compared to the one which is obtained with the gate combination [$E_{\text{int},1} > 30 \text{ keV}$ OR $E_{\text{int},2} > 30 \text{ keV}$ OR $\Delta\theta < 40^\circ$ OR $FM < 0.01$], in Fig. 9. Apart from the reduction of the neutron-induced peaks, e.g. the peaks at 596 keV, 834 keV, 1040 keV, and 1204 keV, and in their associated bumps, the overall background is also reduced successfully in the spectrum produced by this gate combination.

An interesting question is how much the neutron-induced background is removed in the γ -ray spectra produced by standard tracking and by tracking with neutron rejection, compared to the core-energy spectra. A comparison between these three spectra is shown in Fig. 10 and quantitative results are given in Table 4. As mentioned in section 3.2.1, a spectrum created by standard tracking already rejects a considerable amount of the neutron-induced events compared to a core-energy spectrum (see row 1 in Table 4). By using tracking with neutron rejection the spectra are further improved (row 3 in Table 4): the number of counts in the 1040 keV peak is reduced by 69 %, its bump by 72 % and the total ^{252}Cf γ -ray spectrum by 83 % compared to the core-energy spectrum. This loss of counts in the 1332 keV peak of ^{60}Co was in this case 19 % compared to the spectrum obtained by standard tracking and 26 % compared to the core-energy spectrum.

Table 2: Reduction of the number of counts (in percent) in experimental tracked γ -ray spectra when applying different combinations of the neutron- γ discrimination gates. Errors given are purely statistical. See text for details.

Gate	^{252}Cf			^{60}Co	
	1040 keV		Total 0-4095 keV	1173 keV	1332 keV
	peak	peak + bump			
$E_{\text{int},1} > 45 \text{ keV}$	2(3)	16(3)	7.2(1)	4.7(6)	3.9(6)
$E_{\text{int},2} > 45 \text{ keV}$	4(3)	9(3)	5.7(1)	5.1(7)	4.9(6)
$\Delta\theta < 40^\circ$	9(3)	13(3)	6.8(1)	6.7(6)	7.2(6)
$FM < 0.01$	18(3)	23(3)	25.3(1)	9.8(6)	10.2(6)
$E_{\text{int},1} > 30 \text{ keV}$ OR $\Delta\theta < 40^\circ$	10(2)	21(3)	10.4(1)	8.6(6)	8.9(6)
$E_{\text{int},2} > 30 \text{ keV}$ OR $\Delta\theta < 40^\circ$	11(3)	20(3)	9.9(1)	9.6(6)	9.9(6)
$E_{\text{int},1} > 40 \text{ keV}$ OR $E_{\text{int},2} > 40 \text{ keV}$ OR $\Delta\theta < 40^\circ$ OR $FM < 0.01$	28(3)	42(2)	35.4(1)	19.9(6)	20.1(6)
$E_{\text{int},1} > 30 \text{ keV}$ OR $E_{\text{int},2} > 30 \text{ keV}$ OR $\Delta\theta < 40^\circ$ OR $FM < 0.01$	28(3)	42(3)	33.7(1)	18.0(6)	18.5(6)

Table 3: Reduction of the number of counts (in percent) in GEANT4 simulated tracked γ -ray spectra when applying different combinations of the neutron- γ discrimination gates and by using two different low-energy thresholds, 5 keV and 10 keV, on the interaction point energies. Errors given are purely statistical.

	Gate	^{252}Cf			1332 keV
		1040 keV		Total 0-4095 keV	
		peak	peak + bump		
$E_{\text{int, thr}} = 5 \text{ keV}$	$E_{\text{int},1} > 45 \text{ keV}$	2(5)	20(4)	15.2(4)	2(2)
	$E_{\text{int},2} > 45 \text{ keV}$	12(5)	30(4)	22.5(4)	8(3)
	$\Delta\theta < 40^\circ$	6(5)	13(4)	15.4(4)	3(2)
	$FM < 0.01$	16(5)	26(4)	25.7(4)	5(2)
	$E_{\text{int},1} > 30 \text{ keV}$ OR $\Delta\theta < 40^\circ$	8(5)	26(4)	25.5(4)	4(2)
	$E_{\text{int},2} > 30 \text{ keV}$ OR $\Delta\theta < 40^\circ$	14(5)	38(4)	31.1(4)	5(3)
	$E_{\text{int},1} > 30 \text{ keV}$ OR $E_{\text{int},2} > 30 \text{ keV}$ OR $\Delta\theta < 40^\circ$ OR $FM < 0.01$	28(5)	57(4)	51.3(4)	13(2)
$E_{\text{int, thr}} = 10 \text{ keV}$	$E_{\text{int},1} > 45 \text{ keV}$	1(4)	10(3)	9.2(4)	2(4)
	$E_{\text{int},2} > 45 \text{ keV}$	10(4)	17(3)	16.0(4)	7(4)
	$\Delta\theta < 40^\circ$	7(4)	10(3)	14.5(4)	3(4)
	$FM < 0.01$	14(4)	18(3)	22.3(4)	5(4)
	$E_{\text{int},1} > 30 \text{ keV}$ OR $\Delta\theta < 40^\circ$	7(4)	15(3)	20.2(4)	4(4)
	$E_{\text{int},2} > 30 \text{ keV}$ OR $\Delta\theta < 40^\circ$	12(4)	22(3)	24.0(4)	5(4)
	$E_{\text{int},1} > 30 \text{ keV}$ OR $E_{\text{int},2} > 30 \text{ keV}$ OR $\Delta\theta < 40^\circ$ OR $FM < 0.01$	25(4)	39(3)	42.5(4)	12(4)

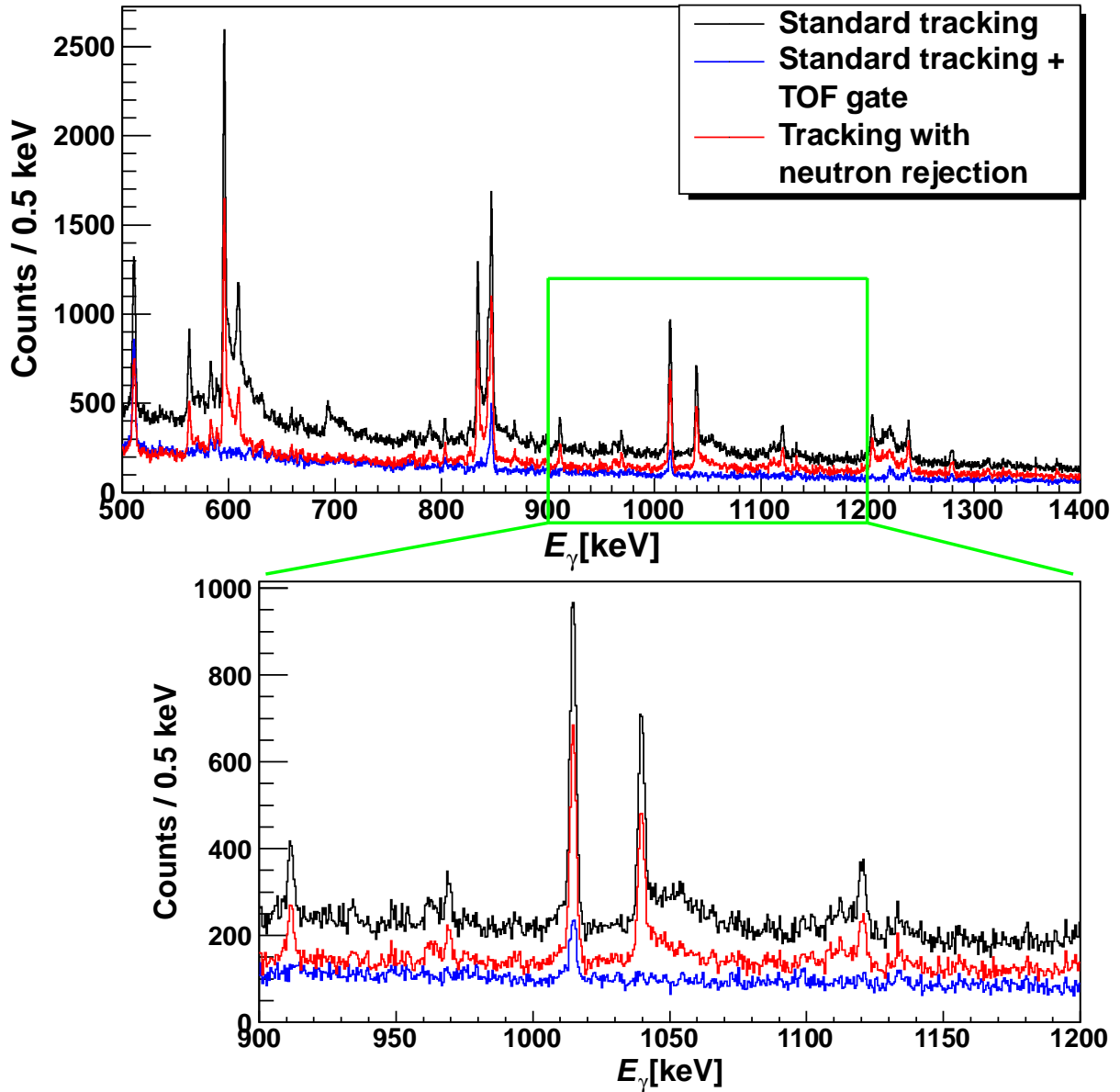


Figure 9: (Colour online) Tracked γ -ray energy spectra obtained with the ^{252}Cf source and by using standard tracking (black), standard tracking + TOF gate on γ rays (blue), and tracking with neutron rejection using the gate combination $[E_{\text{int},1} > 30 \text{ keV OR } E_{\text{int},2} > 30 \text{ keV OR } \Delta\theta < 40^\circ \text{ OR } FM < 0.01]$ (red). The spectra are shown in the energy range where most of the peaks due to inelastic scattering of neutrons in the HPGe crystals are located. An expanded version of the region around the 1040 keV peak ($2^+ \rightarrow 0^+$ transition in ^{70}Ge) is also shown.

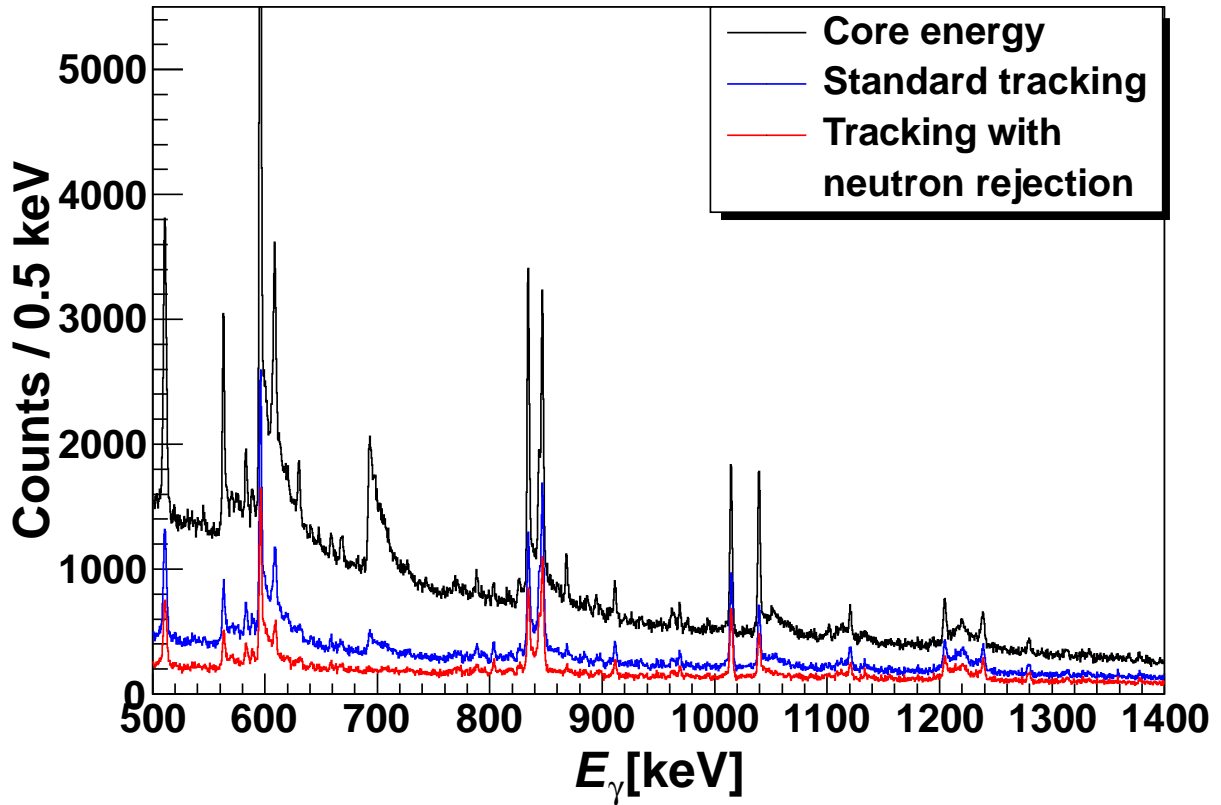


Figure 10: (Colour online) Gamma-ray energy spectra measured with the ^{252}Cf source and displayed in the energy range where most of the peaks due to inelastic scattering of neutrons in the HPGe crystals are located. The following spectra are shown: core-energy spectrum (black), tracked spectrum obtained by standard tracking (blue) and tracked spectrum with neutron rejection (red), using the gate combination $[E_{\text{int},1} > 30 \text{ keV OR } E_{\text{int},2} > 30 \text{ keV OR } \Delta\theta < 40^\circ \text{ OR } FM < 0.01]$.

Table 4: Reduction of the number of counts (in percent) in a spectrum obtained by standard tracking and in a spectrum obtained by using tracking with neutron rejection compared to a core-energy spectrum. The gate used for the spectrum made by tracking with neutron rejection was $[E_{\text{int},1} > 30 \text{ keV OR } E_{\text{int},2} > 30 \text{ keV OR } \Delta\theta < 40^\circ \text{ OR } FM < 0.01]$. Results are shown for the 1040 keV peak, for 1040 keV peak plus its associated bump and for the total spectrum (0-4095 keV) obtained with the ^{252}Cf source, as well as for the 1173 keV and 1332 keV obtained with the ^{60}Co source.

Compared spectra	^{252}Cf			^{60}Co	
	1040 keV		Total 0-4095 keV	1173 keV	1332 keV
	peak	peak + bump			
core energy vs standard tracking	57(1)	52(1)	73.73(2)	11.7(6)	9.0(6)
standard tracking vs tracking with neutron rejection	28(2)	42(2)	33.68(8)	18.0(6)	18.5(6)
core energy vs tracking with neutron rejection	69(1)	72(1)	82.58(2)	27.6(5)	25.8(5)

4. Summary and conclusions

In this work, γ rays originating from inelastic scattering of neutrons from a ^{252}Cf source, which was placed at a distance of 50 cm from four AGATA Triple Cluster detectors, were identified and rejected from tracked γ -ray energy spectra. Several methods for neutron rejection, based on γ -ray tracking and developed in a GEANT4 simulation work [8], were tested with experimental data. The methods were optimised with a special emphasis on not reducing the full-energy peak efficiency of the γ rays of interest.

A time-of-flight measurement, using 16 HELENA BaF₂ detectors as time reference, was performed. This was done in order to have an independent and well understood discrimination of neutrons and γ rays as well as to study the possibility of using TOF discrimination with AGATA. We have shown that the TOF discrimination of neutrons and γ rays, emitted by a ^{252}Cf source, works very well for an ATC to source distance of 50 cm or larger. However, at the nominal ATC to source distance of 23.5 cm or at shorter distances, the TOF discrimination will be of limited use with the presently achievable time resolution of the HPGe detectors. In such cases, the tracking methods for neutron rejection, developed in the previous work [8] and tested here, may be important tools for neutron- γ discrimination.

The standard γ -ray tracking method eliminates effectively most of the interaction points that are due to the recoiling Ge nuclei after elastic scattering of neutrons. Apart from this, standard tracking reduces also the background due to inelastic scattering of neutrons. For example, the 1040 keV peak, which originates from the $^{70}\text{Ge}(n,n'\gamma)$ reaction, was reduced by 57 %, the counts in this peak and its associated bump, due to the summing of the Ge-recoil energies, by 52 % and the total spectrum from 0 keV to 4095 keV by 74 %, as compared to the a γ -ray energy spectrum created from the individual HPGe core signals. In the measurement with a ^{60}Co source, standard tracking caused a loss of 9 % of the counts in the 1332 keV peak compared to the core-energy spectrum.

Further discrimination of neutron-induced events was achieved by using the tracking-based neutron rejection methods. With the combined condition [$E_{\text{int},1} < 30$ keV OR $E_{\text{int},2} < 30$ keV OR $\Delta\theta > 40^\circ$ OR $FM > 0.01$] on the first and second interaction point energies ($E_{\text{int},1}$, $E_{\text{int},2}$), on the difference in the evaluated incoming direction of the γ ray ($\Delta\theta$), or on the figure-of-merit value of the tracking algorithm, the following results were obtained: the 1040 keV

transition was reduced by 28 %, the 1040 keV transition together with its bump by 42 % and the total spectrum from 0 keV to 4095 keV by 34 %, compared to a spectrum obtained by standard tracking. This caused a loss of 19 % of the counts in the 1332 keV peak compared to standard tracking.

The experimental results for tracking with neutron rejection are in reasonably good agreement with the GEANT4 AGATA simulations. It is expected that the results will be improved even further by reducing the low-energy thresholds of the ATC detectors and by improving the pulse-shape analysis techniques for better interaction position resolution.

5. Acknowledgments

This work was partly supported by the Scientific and Technological Council of Turkey (project number 106T055) and by the Swedish Research Council.

References

- [1] S. Akkoyun et al., Nucl. Instr. Meth. A 668 (2012) 26–58.
- [2] M. A. Deleplanque et al., Nucl. Instr. Meth. A 430 (1999) 292–310.
- [3] I. Y. Lee, M. A. Deleplanque, and K. Vetter, Rep. Prog. Phys. 66 (2003) 1095.
- [4] I. Y. Lee et al., Nucl. Phys. A 746 (2004) 255–259.
- [5] S. Agostinelli et al., Nucl. Instr. Meth. A 506 (2003) 250–303.
- [6] E. Farnea et al., Nucl. Instr. Meth. A 621 (2010) 331–343.
- [7] J. Ljungvall and J. Nyberg, Nucl. Instr. Meth. A 550 (2005) 379–391.
- [8] A. Ataç et al., Nucl. Instr. Meth. A 607 (2009) 554–563.
- [9] J. Ljungvall and J. Nyberg, Nucl. Instr. Meth. A 546 (2005) 553–573.
- [10] D. G. Jenkins et al., Nucl. Instr. Meth. A 602 (2009) 457–460.
- [11] I. Abt et al., Eur. Phys. J. A 36 (2008) 139–149.
- [12] A. Gadea et al., Nucl. Instr. Meth. A 654 (2011) 88–96.
- [13] E. Farnea, AIP Conf. Proc. 1491 (2012) 42.
- [14] A. Wiens et al., Nucl. Instr. Meth. A 618 (2010) 223–233.
- [15] C. Boiano et al., IEEE Nucl. Sci. Symp. Conf. Rec. (2008) N30–46.
- [16] R. Venturelli and D. Bazzacco, INFN-LNL Annual Report 2004, INFN-LNL (2005) 220.
- [17] B. Bruyneel, AGATA Detector Simulation Software ADL, <http://www.ikp.uni-koeln.de/research/agata/download.php>, unpublished.
- [18] D. Bazzacco, Nucl. Phys. A 746 (2004) 248–254.
- [19] G. J. Schmid et al., Nucl. Instr. Meth. A 430 (1999) 69–83.
- [20] A. Lopez-Martens et al., Nucl. Instr. Meth. A 533 (2004) 454–466.
- [21] D. C. Radford, GF3 program, <http://radware.phy.ornl.gov/>, unpublished.

- [22] R. Brun and F. Rademakers, Nucl. Instr. Meth. A 389 (1997) 81 – 86.
- [23] G. F. Knoll, Radiation Detection and Measurement, John Wiley & Sons, Inc., fourth edition edition (2010), and references therein.
- [24] T. E. Valentine, Ann. Nucl. Energy 28 (2001) 191 – 201, and references therein.
- [25] D. L. Bleuel et al., Nucl. Instr. Meth. A 624 (2010) 691 – 698.
- [26] N. Ensslin, Passive Nondestructive Assay of Nuclear Materials, Los Alamos National Laboratory (1991) 337 – 356, <http://www.fas.org/sgp/othergov/doe/lanl/lib-www/la-pubs/00326406.pdf>.
- [27] Q. B. Shen, CENDL-3.1 MAT 3200 (September 2002).
- [28] O. Iwamoto et al., ENDF/B-VII MAT 3225 (August 2004).
- [29] M. S. Basunia, Nucl. Data Sheets 112 (2011) 1875 – 1948.
- [30] D. V. Elenkov, D. P. Lefterov, and G. H. Toumbev, J. Phys. G: Nucl. Phys. 8 (1982) 997–1005.
- [31] F. C. L. Crespi et al., Nucl. Instr. Meth. A 620 (2010) 299 – 304.
- [32] F. Recchia et al., Nucl. Instr. Meth. A 604 (2009) 60 – 63.
- [33] F. Recchia et al., Nucl. Instr. Meth. A 604 (2009) 555 – 562.